ASME 2012 5th Annual Dynamic Systems and Control Conference joint with the JSME 2012 11th Motion and Vibration Conference
DSCC2012-MOVIC2012
October 17-19, 2012, Fort Lauderdale, Florida, USA

DSCC2012-MOVIC2012-8539

DECENTRALIZED VOLTAGE CONTROL TO MINIMIZE DISTRIBUTION LOSSES IN AN ISLANDED MICROGRID

Changsun Ahn
Department of Mechanical Engineering
University of Michigan
Ann Arbor, MI 48109
sunahn@umich.edu

Huei Peng
Department of Mechanical Engineering
University of Michigan
Ann Arbor, MI 48109
hpeng@umich.edu

ABSTRACT

Microgrids can bring electricity power to rural communities or isolated military forward operation bases. For many rural areas, renewable powers could be the cheapest power sources available. Utilizing renewable power sources and energy storage systems such as batteries requires new power and voltage control strategies. In addition, these microgrids may be reconfigured frequently. Therefore, the control strategies must be implemented in a plug-and-play fashion at individual nodes, and ideally they should not require much communication with neighboring nodes. Another issue of microgrids is the resistance loss in distribution lines due to the lower operating voltage. To reduce power losses, voltage control is required which again must work in a plug-and-play fashion. In this paper, we propose a decentralized real-time voltage control algorithm that minimizes power losses for a microgrid supported by inverter based distributed power sources. Its optimality and plug-and-play nature are demonstrated through simulations.

INTRODUCTION

Distributed renewable power sources are increasingly used because of the push for low carbon electricity. They were treated as "negative loads" in the past but will need to be treated as intermittent supplies when they provide a significant portion of the grid power. The intermittency can cause grid instability if inadequate reserve and regulation services are not present. The intermittency problem is more profound for microgrids relying on renewable power sources [1-4]. For military applications, the microgrid concept is especially appealing considering energy security and independence. In this paper, we will focus on microgrids that are islanded, i.e., not connected to the mega grid. In these microgrids, it is desirable to deploy renewable energy sources such as solar and wind to reduce reliance on fossil fuels. In addition, electrified vehicles can play an important role using vehicle-to-grid (V2G) technologies [5-7]. For these military applications, it makes sense to use the batteries and engines of electrified vehicles to support the microgrid and explore their synergistic design and usage for improved overall grid efficiency.

Islanded microgrids have much smaller inertia than the conventional grids. For distributed power sources supported by inverters, there may not exist any inertia at all. In such cases, regulating the grid frequency becomes challenging and a number of control strategies have been studied [8-11]. Another important attribute of islanded microgrids is that the lower operation voltage results in high distribution losses than on high voltage grids. Voltage or reactive power allocation over the microgrid network can be used to reduce distribution losses.

In conventional grid systems, voltage/reactive power allocation is determined through optimization using the knowledge of the grid structure and operating conditions [12-15]. A few approaches were suggested to determine the optimal voltage profiles in real-time, but they require the knowledge of the grid structure [16] and typically require a centralized implementation [17]. For microgrids, the control strategy must be plug-and-play because the frequent reconfiguration. In addition, it is desirable to develop a control algorithm that requires limited communications and measurements. New load and supply nodes could be added, i.e., the grid configuration can change and may not be known to the control algorithm. The main contribution of this paper is a model-

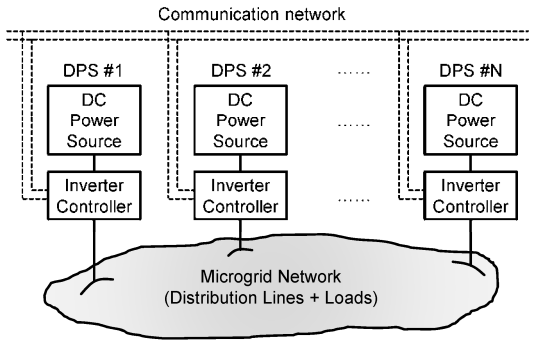

FIGURE 1. STRUCTURE OF THE MICROGRID SUPPORTED BY DISTRIBUTED DC POWER SOURCES.

free, distributed voltage control algorithm for islanded microgrids that minimizes distribution losses.

This "plug-and-play" control algorithm consists of two levels. The low level control regulates the power output and the terminal voltage to follow the set values that are determined by a high level controller. It is designed based on inverter and phase-locked loop (PLL) systems. The high level controller is designed using a cost function on distribution power losses. We derive a condition that guarantees the power loss minimization without requiring central coordination.

DECENTRALIZED CONTROL DESIGN

The structure of the microgrid supported by distributed power sources is shown in Figure 1, where a communication network enables small amount of information sharing. The DC power sources can be solar panels, batteries, or power from wind turbines that has been converted to DC. The detailed view of the controller is shown in Figure 2 where the controller consists of a high level controller, a low level controller, a phase locked loop, and a measurement and computation block.

Low-Level Controllers

The low level controllers consist of servo loops for controlling an inverter. In this section, we describe the inverter and controllers both located in the 'Inverter Controller' block of Figure 1. The inverter model is shown in Figure 3, which consists of a DC to AC converter and an inverter-grid interface. The voltage at the inverter bus is synthesized to an AC voltage wave form and the voltage at the terminal bus is common with the grid side. The primary goals of the inverter are to regulate the terminal bus voltage V_t and the active power delivered to the grid P_{gen}. This is achieved by controlling the modulation index m of the inverter, which controls the inverter voltage V_i through the relationship

$$V_i = mV_{dc}, \tag{1}$$

and the inverter firing angle, which determines the phase angle δ_i. The active power delivered to the grid is then given by

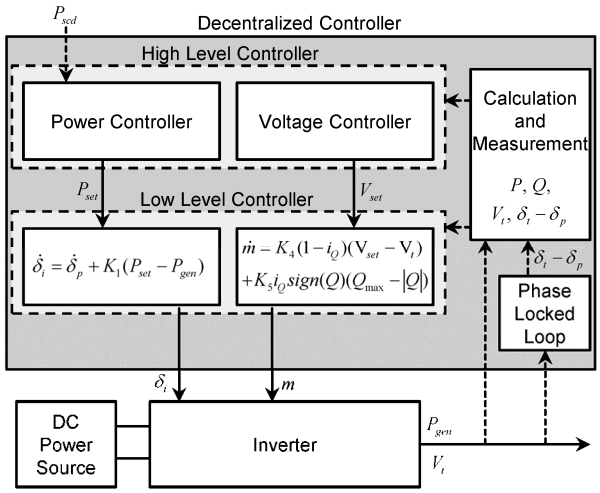

FIGURE 2. STRUCTURE OF THE DECENTRALIZED CONTROLLER AT EACH SOURCE NODE.

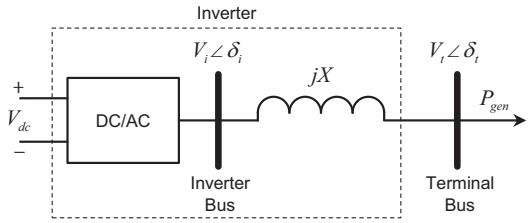

FIGURE 3. INVERTER MODEL

$$P_{gen} = \frac{V_i V_t}{X}\sin(\delta_i - \delta_t). \tag{2}$$

The two control variables, m and δ_i, are controlled by the low level controller shown in Figure 2.

This paper considers low-level control based on the use of a PLL to ensure synchronization to the grid voltage. The active power output is determined by δ_i, and the low-level loop for active power regulation is described by the following equation:

$$\dot{\delta}_i = \omega_p + K_1(P_{set} - P_{gen}), \tag{3}$$

where P_{set} is the desired active power output given by the high level controller, P_{gen} is the active power output, and ω_p is the frequency observed by the PLL. The terminal voltage V_t is regulated by controlling V_i, which can be achieved by the modulation index control:

$$\dot{m} = K_4(1 - i_Q)(V_{set} - V_t) + K_5 i_Q sign(Q)(Q_{\max} - |Q|), \tag{4}$$

where V_{set} is a desired voltage magnitude given by the high level controller, and Q_{max} and i_Q are determined by

$$Q_{\max} = \sqrt{S_{\max}^2 - P^2}, \quad i_q = \begin{cases} 1, & if\ |Q| \geq Q_{\max} \\ 0, & if\ |Q| < Q_{\max} \end{cases}. \tag{5}$$

The first term on the right hand side of Eq. (4) is activated only when the magnitude of the reactive power is lower than Q_{max}, and the voltage is being controlled (voltage control mode).

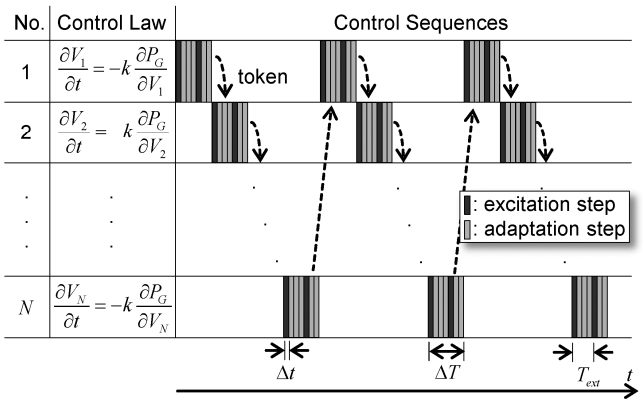

FIGURE 4. CONCEPT OF THE VOLTAGE CONTROL ALGORITHMS

Once the reactive power exceeds Q_{max}, then the second term is activated and reactive power is controlled (reactive power control mode). This discrete control structure enables voltage control while keeping the reactive power within limits.

High-Level Controller

The high level controller determines the desired values for the active power output and the magnitude of the terminal voltage. The active power output should match the load, by regulating the grid frequency. For load sharing, we assume a proportional control is used, as follows:

$$P_{set} = P_0 + K_P \Delta\omega, \tag{6}$$

where P_0 is the preset power, K_P is the proportional (or droop) gain, and $\Delta\omega$ is the frequency error.

In a similar control strategy, the set values of voltage magnitude are determined by the high level voltage controller. The derivation of the high level voltage controller starts from the definition of a cost function, defined as follows:

$$P_{Loss}(\mathbf{V}) = P_G(\mathbf{V}) - P_L = \sum_{i=1}^{N} P_{Gi}(\mathbf{V}) - \sum_{j=1}^{M} P_{Lj}, \tag{7}$$

where, P_{Loss} is the total power loss in the grid, $\mathbf{V}=[V_1, V_2, \cdots, V_N]^T$, P_G is the total power generation, P_{Gi} is the power supplied from the generator bus #i to the grid, and P_{Lj} is the power consumed at the load bus #j which is assumed to be constant or slowly time-varying. N is the number of generator buses and M is the number of load buses. The objective is to minimize the cost function by controlling the voltages at the generator buses, $V_1, V_2, \cdots, V_N$. The voltages should be controlled in a decentralized way with a minimum amount of information flow to facilitate a plug-and-play capability. A condition for monotonically decreasing $P_{Loss}(\mathbf{V})$ is:

$$\frac{\partial P_{Loss}(\mathbf{V})}{\partial t} = \frac{\partial P_G(\mathbf{V})}{\partial t} - \frac{\partial P_L}{\partial t} = \frac{\partial P_G(\mathbf{V})}{\partial t} \le 0, \tag{8}$$

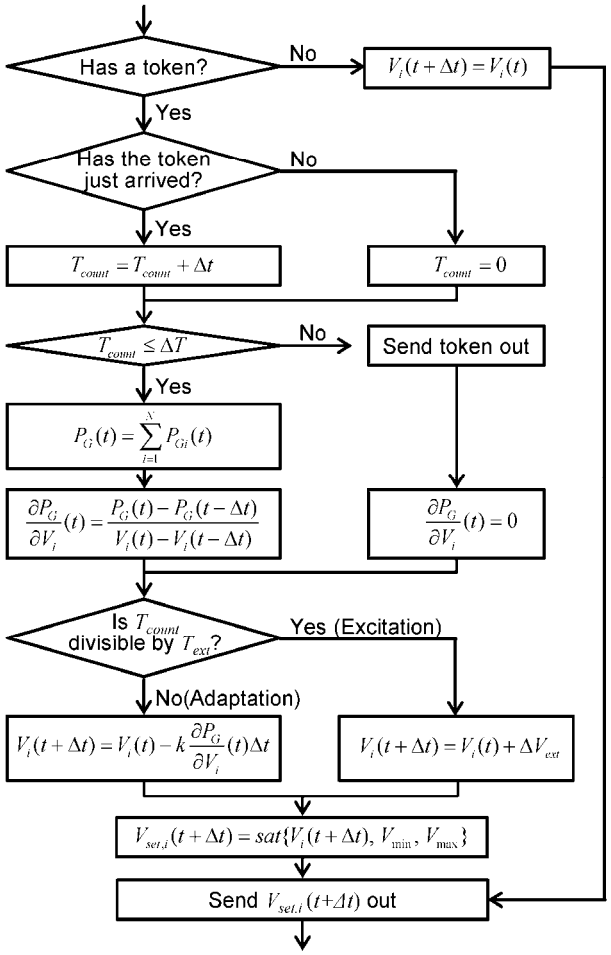

FIGURE 5. FLOW CHART OF THE CONTROL ALGORITHM. T_{count} IS THE TIME COUNTER; Δt IS THE TIME STEP; ΔT IS THE CONTROL TIME SPAN; T_{ext} IS THE EXCITATION PERIOD; ΔV_{ext} IS THE MAGNITUDE OF VOLTAGE EXCITATION; V_{min} IS THE VOLTAGE LOWER LIMIT; AND V_{max} IS THE VOLTAGE UPPER LIMIT.

where the time derivative of P_L is ignored because P_{Lj} is assumed to be slowly time varying. Eq. (8) can be rewritten as:

$$\frac{\partial P_G(\mathbf{V})}{\partial t} = \left(\frac{\partial P_G(\mathbf{V})}{\partial \mathbf{V}}\right)^T \frac{\partial \mathbf{V}}{\partial t} \le 0. \tag{9}$$

If a control law is chosen as follows

$$\frac{\partial \mathbf{V}}{\partial t} = -k\frac{\partial P_G(\mathbf{V})}{\partial \mathbf{V}}, \tag{10}$$

where k is positive real, then Eq. (9) always holds because

$$\frac{\partial P_G(\mathbf{V})}{\partial t} = \left(\frac{\partial P_G(\mathbf{V})}{\partial \mathbf{V}}\right)^T \frac{\partial \mathbf{V}}{\partial t} = -k\left\|\frac{\partial P_G(\mathbf{V})}{\partial \mathbf{V}}\right\|^2 \le 0. \tag{11}$$

The control law Eq. (11) can be implemented without knowing the precise grid structure by measuring $\partial P_G/\partial \mathbf{V}$. However, this algorithm needs to know the total generated

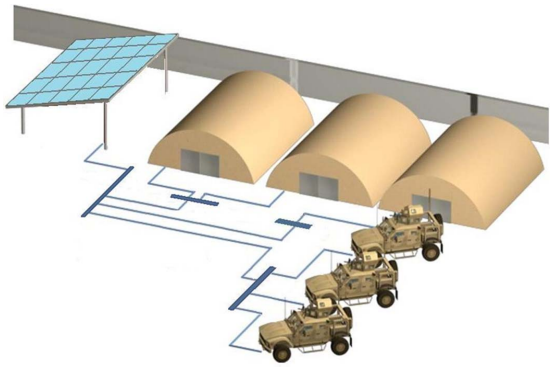

FIGURE 6. AN IMAGINED MILITARY MICROGRID.

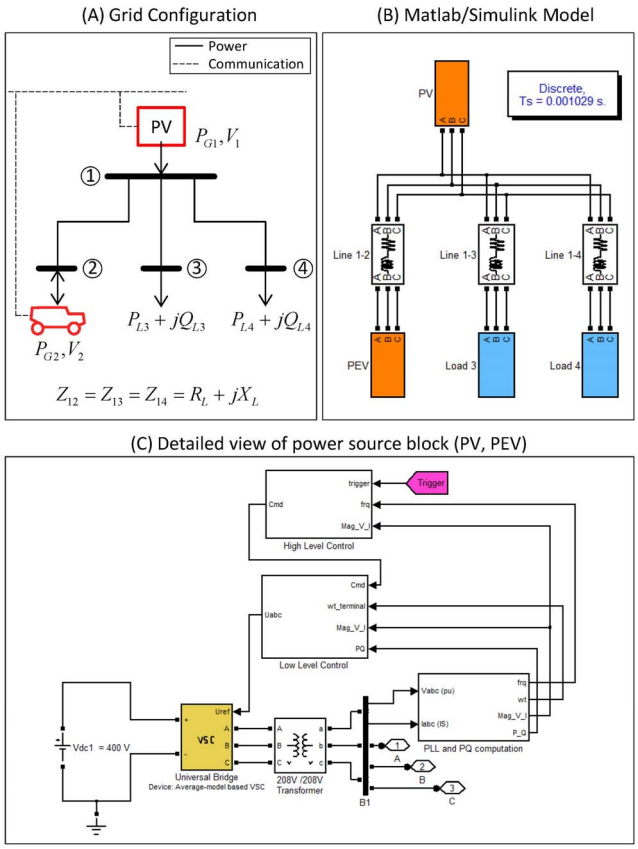

FIGURE 7. (A) GRID MODEL OF THE EXAMPLE SYSTEM SHOWN IN FIG. 5, (B) GRID MODEL IN *MATLAB /SIMULINK® SIMPOWERSYSTEMS*, (C) DC POWER SOURCE AND INVERTER MODELS (PEV, PV BLOCKS).

power. Fortunately, the necessity of the central control authority can be removed by using sequential execution of the voltage control based on a simple communication protocol in a decentralized way by communicating two pieces of information. The first piece is the amount of power generated by all the generators; the information has to be broadcasted. The second piece is a token signal that designates an active voltage controller to realize the sequential execution. Only the

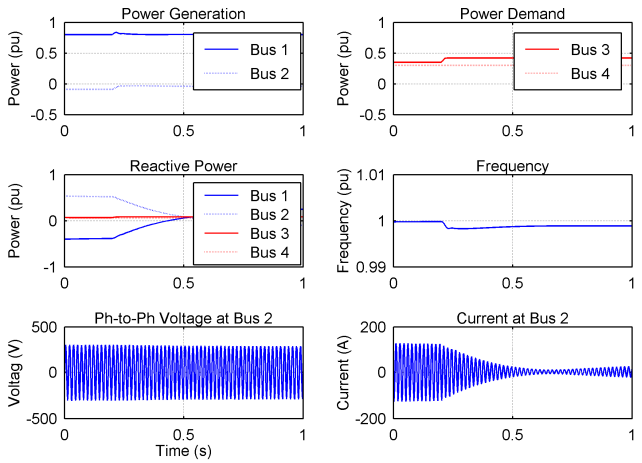

FIGURE 8. SIMULATION OF THE ISLANDED MICROGRID UNDER POWER DEMAND PERTURBATIONS

power source that has the token can adjust its voltage. At each instant, only one power source varies its voltage and calculates the sensitivity. To facilitate the adaptation processes, the control algorithm needs to excite the voltages regularly. The concept is shown in Figure 4 and the algorithm is shown in Figure 5.

SIMULATION STUDY

The proposed control concept was tested with a simulated grid model for a military forward operating base. We assumed that the base has about 50 soldiers and is supported by distributed power sources such as solar panels and electrified vehicles, as shown in Figure 6. This network can be represented as Figure 7 (A) and is modeled using *Matlab/Simulink® SimPowerSystems* simulation platform, as shown in Figure 7 (B). It includes models and controls for PV panels and DC power sources (Plug-in Electric Vehicles) as well as loads. In this specific example, the electricity grid consists of two supply buses and two demand buses. The power from the vehicles was controlled to regulate the frequency. The controller shown in Figure 2 was implemented in every power source in the discrete time, as shown in Figure 7 (C). The grid parameters and the initial conditions are listed in *Appendix*. Under the given condition, the minimum power loss was calculated by offline computation for performance evaluation.

Before we evaluate the performance of the controller, we verify the feasibility of self-sustainable operation of the islanded microgrid supported by distributed power sources under changes of operation conditions. Initially, the total demand of Bus 3 and 4 was 39 kW and increased to 43.2 kW. As a result, the vehicle charging power reduced from 6 kW to 1.8 kW and the magnitude of current reduced to compensate for the demand increases. The frequency dropped as a result and the droop controller reacted to the frequency drop. Corresponding voltage and current trajectories are shown in Figure 8, which shows that the low level controller based on frequency droop effectively deals with power imbalance.

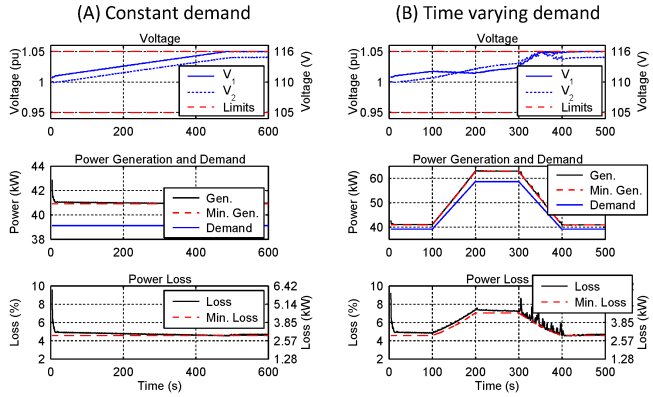

FIGURE 9. PERFORMANCE OF THE VOLTAGE CONTROL IN THE GRID SHOWN IN FIGURE 7 (A) UNDER CONSTANT DEMAND AND (B) UNDER TIME VARYING DEMAND

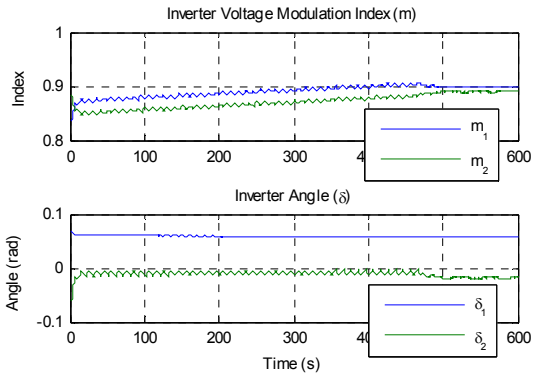

FIGURE 10. CONTROL VARIABLES FOR THE CASE OF CONSTANT DEMAND (FIGURE 9 (A)).

In Figure 9 (a) showing voltage and power loss trajectory for a constant demand case, the power loss reduced quickly at first as the two bus voltages moved away from each other, and then slowly as the two voltage increased together. The controlled voltages, V1 and V2, approached the optimal vales, 1.05 pu and 1.04 pu, where the minimum power loss was computed through exhaustive brutal-force search. Because the power flowed from Bus 1 to Bus 2 and the reactive power flow was quite small, V1 turned out to be higher than V2. The total power loss is reduced from around 9.6% to 4.6%, i.e., by properly setting the voltages of the nodes, the distribution loss is reduced by about 50%, which is quite significant. Corresponding control variables (δ_i and m) are plotted in Figure 10. This level of power loss reduction is achieved mainly because of the fact the voltage level of the microgrid is much lower and the power lines are more resistive than high voltage network. Figure 9 (b) shows the case of a varying demand, where active power and reactive power demand vary simultaneously. From 0 seconds to 100 seconds, V1 was higher than V2 because the power flowed from Bus 1 to Bus 2. However, at 150 seconds, demand increased above the supply

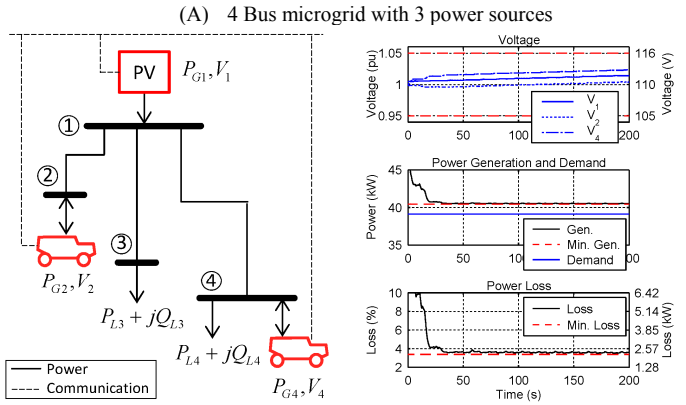

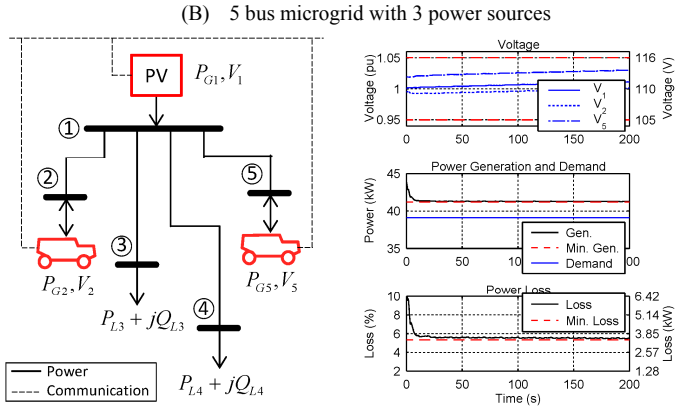

FIGURE 11. SIMULATION RESULTS (A) WHEN A GROUP OF ELECTRIFIED VEHICLES ARE CONNECTED TO BUS 4, (B) WHEN A GROUP OF ELECTRIFIED VEHICLES ARE CONNECTED TO A NEW BUS, BUS 5.

level from the solar panels and the electrified vehicles provided power back to the grid to compensate for the supply shortage. In this situation, because power must flow from Bus 2 to Bus 1, V2 turned out to be higher than V1. Between 300~400 seconds, the power loss did not decreased monotonically because the algorithm did not know whether the power generation reduction was from proper voltage set values or from the power demand decreases. However, the algorithm brought the power loss level back to the minimum level as soon as the power demand became slowly time varying. Between 400~500 seconds, the bus voltages returned to that before the demand increase. The results show that the decentralized controller works well without the knowledge of the operating conditions.

The scalability and flexibility of the control algorithm were tested using different grid configurations. Distributed power sources, especially electrified vehicles, can be relocated to other Buses due to mission requirement which can modify the grid configuration. Figure 11 and 12 show the performance of the voltage controller under changing grid structures. In the case of Figure 11 (a), a fleet of vehicles was connected to Bus 4 and supplied power to the grid. As a result, three controllable voltages changed to achieve the minimum power loss. Similar

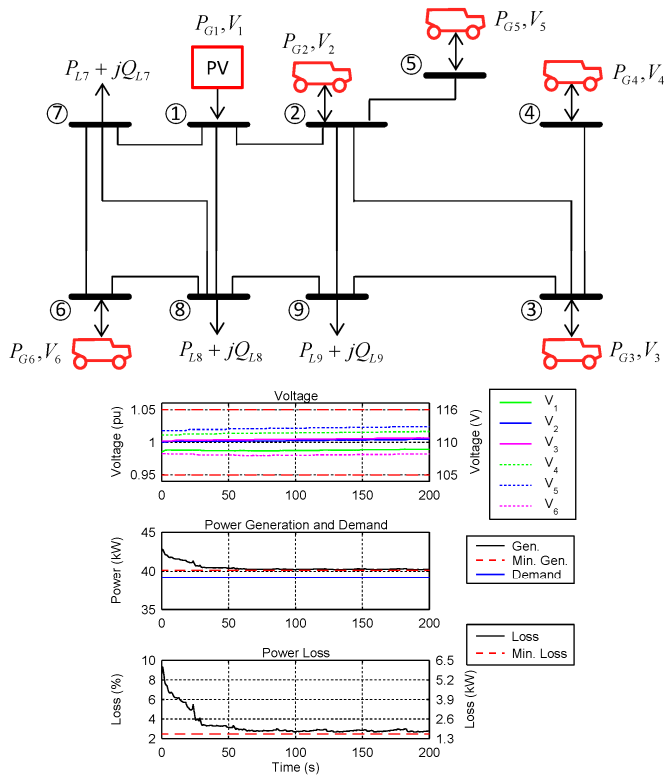

FIGURE12. SIMULATION WHEN FIVE BUSES ARE CONNECTED WITH VEHICLES AND ONE BUS IS

to the previous cases, the power loss quickly reduced as soon as the control started and slowly approached the minimum value. In this case, the power loss was reduced to 3.4% because the newly connected vehicle supplied power to the load directly. In the case of Figure 11 (b), the vehicle that was connected to Bus 4 moved to a new bus, Bus 5. The overall control characteristics are similar to the previous cases. In the case of Figure 12 where the grid has nine buses, the voltages of the buses with power sources again varied according to the control law and achieved minimum power losses automatically. As the control variables increase the convergence to the minimum condition takes more time than cases of Figure 11 because of the higher complexity. These three tests indicate that the algorithm can adapt to grid structure changes and work in a plug-and-play fashion reliably.

CONCLUSION

A microgrid is an attractive concept to incorporate renewable power sources. However, it requires new control strategies for power outputs and terminal voltages of power sources. Military microgrids, which have a flexible grid structure and are operated in a low voltage level, require a voltage control algorithm that works in a plug-and-play way. In this paper, we proposed a decentralized controller that is derived from a cost function and minimizes power loss over the grid network. Computer based simulation showed that the algorithm can work without knowledge of different operating conditions and grid structures under the slowly time varying power demand conditions.

ACKNOWLEDGMENTS

The financial support for this research is provided by the Automotive Research Center (ARC), a U.S. Army Center of Excellence in Modeling and Simulation of Ground Vehicles.

APPENDIX

TABLE 1. GRID PARAMETERS

Symbol	Value	Unit	Description
R_L	0.1	pu	Line resistance
X_L	0.01	pu	Line reactance

All distribution lines are assumed to be identical. The base voltage is 110V, the base power is 60kW.

TABLE 2. INITIAL CONDITIONS FOR GRID OF FIGURE 6

Symbol	Value	Unit	Description
P_{L3}, P_{L4}	0.35, 0.3	pu	Active power demand at Bus 3 and 4, constant
Q_{L3}, Q_{L4}	0.07, 0.06	pu	Reactive power demand at Buses 3 and 4, constant
P_{G1}	0.8	pu	Power from PV, constant, and uncontrollable
P_{G2}	-0.1	pu	Power from vehicles, varying, and controllable
V_1, V_2	1.0, 1.0	pu	Terminal voltages of Buses 1 and 2, varying, and controllable

The base voltage is 110V, the base power is 60kW. P_{G2}, V_1, and V_2 vary as the controllers are engaged.

REFERENCES

[1] R. Lasseter, A. Akhil, C. Marnay, J. Stephens, J. Dagle, R. Guttromson, A. S. Meliopoulous, R. Yinger, and J. Eto, "Integration of distributed energy resources: The CERTS microgrid concept," U.S. Department of Energy and California Energy Commission, LBNL-50829, 2002.

[2] R. H. Lasseter and P. Paigi, "Microgrid: a conceptual solution," in *IEEE Power Electronics Specialists Conference*, Aachen, Germany, 2004, pp. 4285-4290 Vol.6.

[3] N. Hatziargyriou, H. Asano, R. Iravani, and C. Marnay, "Microgrids," *IEEE Power and Energy Magazine,* vol. 5, pp. 78-94, 2007.

[4] J. M. Guerrero, "Microgrids: Integration of distributed energy resources into the smart-grid," in *IEEE International Symposium on Industrial Electronics*, Bari, Italy, 2010, pp. 4281-4414.

[5] W. Kempton and J. Tomic, "Vehicle-to-grid power implementation: From stabilizing the grid to supporting

large-scale renewable energy," *Journal of Power Sources,* vol. 144, pp. 280-294, 2005.
[6] T. Ersal, C. Ahn, I. A. Hiskens, H. Peng, and J. L. Stein, "Impact of controlled plug-in EVs on microgrids: a military microgrid example," in *IEEE Power & Energy Society General Meeting*, 2011.
[7] C. Ahn, C.-T. Li, and H. Peng, "Optimal decentralized charging control algorithm for electrified vehicles connected to smart grid," *Journal of Power Sources,* vol. In Press, Corrected Proof.
[8] K. De Brabandere, B. Bolsens, J. Van den Keybus, A. Woyte, J. Driesen, R. Belmans, and K. U. Leuven, "A voltage and frequency droop control method for parallel inverters," in *IEEE Power Electronics Specialists Conference*, Aachen Germany, 2004, pp. 2501-2507 Vol.4.
[9] A. Engler and N. Soultanis, "Droop control in LV-grids," in *International Conference on Future Power Systems*, Amsterdam, The Netherlands, 2005, pp. 6 pp.-6.
[10] M. Tokudome, K. Tanaka, T. Senjyu, A. Yona, T. Funabashi, and K. Chul-Hwan, "Frequency and voltage control of small power systems by decentralized controllable loads," in *International Conference on Power Electronics and Drive Systems*, Taipei, Taiwan, 2009, pp. 666-671.
[11] J. M. Guerrero, J. C. Vasquez, J. Matas, L. G. de Vicuna, and M. Castilla, "Hierarchical control of droop-controlled AC and DC microgrids-A general approach toward standardization," *IEEE Transactions on Industrial Electronics,* vol. 58, pp. 158-172, Jan 2011.
[12] A. Kishore and E. F. Hill, "Static optimization of reactive power sources by use of sensitivity parameters," *IEEE Transactions on Power Apparatus and Systems,* vol. PAS-90, pp. 1166-1173, 1971.
[13] D. T. W. Sun and R. R. Shoults, "A preventive strategy method for voltage and reactive power dispatch," *IEEE Transactions on Power Apparatus and Systems,* vol. PAS-104, pp. 1670-1676, 1985.
[14] S. Granville, "Optimal reactive dispatch through interior point methods," *IEEE Transactions on Power Systems,* vol. 9, pp. 136-146, 1994.
[15] H. Yoshida, K. Kawata, Y. Fukuyama, S. Takayama, and Y. Nakanishi, "A particle swarm optimization for reactive power and voltage control considering voltage security assessment," *IEEE Transactions on Power Systems,* vol. 15, pp. 1232-1239, 2000.
[16] K. Tanaka, T. Senjyu, S. Toma, A. Yona, T. Funabashi, and K. Chul-Hwan, "Decentralized voltage control in distribution systems by controlling reactive power of inverters," in *IEEE International Symposium on Industrial Electronics*, Seoul, Korea, 2009, pp. 1385-1390.
[17] A. Cagnano, E. De Tuglie, M. Liserre, and R. Mastromauro, "On-line optimal reactive power control strategy of PV-inverters," *IEEE Transactions on Industrial Electronics,* vol. PP, pp. 1-1, 2011.